

DOI: 10.24425/amm.2019.127613

J. BARCZYK^{*#}, G. DERCZ^{*#}, I. MATUŁA^{*}, M. GÓRAL^{**}, J. MASZYBROCKA^{*},
D. BOCHENEK^{***}, W. GURDZIEL^{*}**MICROSTRUCTURE AND PROPERTIES OF YSZ COATINGS PREPARED BY PLASMA SPRAY PHYSICAL VAPOR DEPOSITION FOR BIOMEDICAL APPLICATION**

This paper presents the study of microstructure and properties of 8 mol% yttrium stabilized zirconia coating fabricated by Plasma Spray Physical Vapor Deposition technique on commercial pure titanium. The coating was characterized by X-ray diffraction, high resolution scanning electron microscope, profilometer, nanoindentation and nanomachining tests. The X-ray phase analysis exhibit the tetragonal $Zr_{0.935}Y_{0.065}O_{1.968}$, TiO and α -Ti phases. The Rietveld refinement technique were indicated the changes of crystal structure of the produced coatings. The characteristic structure of columns were observed in High Resolutions Scanning Electron Microscopy. Moreover, the obtained coating had various development of surfaces, thickness was equal to 3.1(1) μm and roughness 0.40(7) μm . Furthermore, the production coatings did not show microcracks, delamination and crumbing. The performed experiment encourages carried out us to tests for osseointegration.

Keywords: PS-PVD method, bioactive coatings, cp-Ti, YSZ, osseointegration

1. Introduction

Recently, the bioactive coatings on the metal substrate have focused the attention of researchers. The material often used as coating is Yttrium Stabilized Zirconium (YSZ) because it has attractive properties such as chemical stability and exhibits a slight effect on inflammation at the implant site [1,2]. As a substrate, commercial pure titanium (cp-Ti) is frequently used. The modification of cp-Ti is needed to improve its features such as poor tribological properties, and to improve the osseointegration between implants and human bone and to reduce the Young's modulus [3-5].

Nowadays, a variety of methods is used to make coatings on titanium-based substrates, e.g.: the Electron Beam Physical Vapor Deposition (EB-PVD), Plasma Electrotype Oxidation (PEO) or Air Plasma Spraying (APS). Unfortunately, regardless of the method used, each coatings had various defects i.e. microcracks and delamination. As an alternative to the above, in this work a YSZ coating was produced by Plasma Spray – Physical Vapor Depositions (PS-PVD) method. This method allows to obtain optimal roughness and thickness for better osseointegration with characteristic columnar structure of coatings [6]. Currently the method is widely used in the aviation industry [7,8].

In this work a ceramic coating was produced with 8% mole YSZ sprayed on commercially pure titanium with of PS-PVD method. The main goal of these researches was to determinate

the microstructure and different properties of coating for potential biomedical application.

2. Experimental

The rode shape cp-Ti was used as a substrate. The coating was obtained in LPPS-Hybrid Oerlikon Metco by PS-PVD (Plasma Spray Physical Vapor Deposition) method. The 8 %mol YSZ (MetcoTM 6700, Oerlikon) was applied in the feedstock. The basic process parameters used to perform the experiment: chamber pressure 1.5 mBa, sample rotation 20 rpm, plasma gasses He60/Ar35 NLPM, current 2400 A, powder feeding rate of 2 g/min, time of spraying 400 s. The process was carried out using plasma gun 03CP type and powder feeder 60CD.

The phase composition of the coating was studied by X-ray diffraction (XRD) method. The measurements were performed with an X-ray X'Pert diffractometer (Phillips), with a copper anode lamp ($\text{Cu}_{K\alpha} - \lambda = 1.54178 \text{ \AA}$) powered by an electric current of 30 mA and a voltage of 40 kV, and a curved graphite monochromator to determine the wavelengths emitted from the copper anode. The diffraction patterns were recorded by "step-scanning" of 0.04 $^{\circ}2\theta$ steps through an angle range from 10 $^{\circ}2\theta$ to 140 $^{\circ}2\theta$.

Rietveld's method was applied for the structure analysis. To examine the surface of the coatings and to illustrate the column

* UNIVERSITY OF SILESIA IN KATOWICE, INSTITUTE OF MATERIALS SCIENCE, 75 PUŁKU PIECHOTY 1A, 41-500 CHORZÓW, POLAND

** RZESZOW UNIVERSITY OF TECHNOLOGY, DEPARTMENT OF MATERIALS SCIENCE, 8 POWSTAŃCÓW WARSZAWY AV., 35-959 RZESZÓW, POLAND

*** UNIVERSITY OF SILESIA IN KATOWICE, INSTITUTE OF TECHNOLOGY AND MECHATRONICS, 12 ZYTANIA STR., POLAND

Corresponding authors: jbarczyk@us.edu.pl, grzegorz.dercz@us.edu.pl

structure (cross-section), High Resolution Scanning Electron Microscope JOEL JMS-7100F TTL LV with accelerating voltage of 15 kV was applied. The base of profile parameters of produced coatings was measured by profilometer Mitutoyo SURFTTEST SJ-500. To define hardness parameters and Young's modulus the Hysitron TI 950 triboindenter was used.

3. Results and discussion

Fig. 1 shows X-ray diffraction patterns for obtained samples. The analysis reveals the presence of three phases: tetragonal $Zr_{0.935}Y_{0.065}O_{1.968}$, TiO and α -Ti. The presence of the TiO phase is most likely caused by the oxidation of the substrate during deposition of coating. On the basis of XRD analyzes, the lattice parameters were determined using the Rietveld method. All parameters for individual phases together with data from the ICDD database are presented in Table 1. The a_0 parameter of the $Zr_{0.935}Y_{0.065}O_{1.968}$ phase lattice parameter was 0.36214(3) nm and b_0 was 0.51607(7) nm. According to the ICDD database, the a_0 parameter for $Zr_{0.935}Y_{0.065}O_{1.968}$ phase shows a slight increase but c_0 has decreased to 0.46801(7). Probably the change in value

is the result of the reduction of the elementary unit cell during the deposition process. However, in case of α -Ti phase no changes in the value in the lattice parameter were observed. It is worth mentioning, in the case of the TiO phase, that the parameter increased from the ICDD (International Centre for Diffraction Data) reference value to 0.41973(9) nm.

Fig. 2 shows the cross-sectional microphotograph of the coating. The micrographs show a compact, homogeneous coating well associated with the substrate. The surface microcracks and delamination of the coating are not observed. Additionally, the average thickness of the sprayed YSZ is about 3 μ m. Referring to the thickness of the coating, usually ceramic coatings on implants have different thicknesses depending on the method being used. However, our coating (3.1 μ m) can be classified into one of the thinnest. Based on literature we know that this is a positive aspect because it will reduce the risk of coating crumbling. The different thickness of coatings can also be obtained by PS-PVD method. The high-resolution scanning microscope shows columnar microstructure with gaps between single columns microstructure that is characteristic for materials prepared by the PS-PVD method. The occurrence of these columns is probably related to the so-called shade effect of embedded clusters of particles during the process. This is the interaction between the roughness of the substrate and the deposited particles at a different angle. The shading phenomenon increases with the growing coating. The consequence of this is the column structure of the coating with domed vertices and empty spaces between the columns [9]. The previously mentioned domed tops perfectly show Fig. 3.

TABLE 1

Summary of lattice parameters (a_0 , b_0 , c_0) for individual sample phases determined by the Rietveld method

Phase	Unit-cell parameters [nm]			Type of change
		ICDD*	Ti_2_400	
α Ti	a_0	0.29505	0.29644(6)	○
	c_0	0.46826	0.46801(7)	○
$Zr_{0.935}Y_{0.065}O_{1.968}$	a_0	0.36060	0.36214(3)	⋈
	b_0	0.51800	0.51607(7)	⋈
TiO	a_0	0.41770	0.41973(9)	⋈

* International Centre for Diffraction Data®

TABLE 2

Basic surface parameters with an average thickness for the obtained coating

Sample	Average thickness [μ m]	R_A [μ m]	R_P [μ m]	R_Z [μ m]	R_V [μ m]
Ti_2_400	3.1(1)	0.40(7)	2.6(5)	3.8(6)	1.3(2)

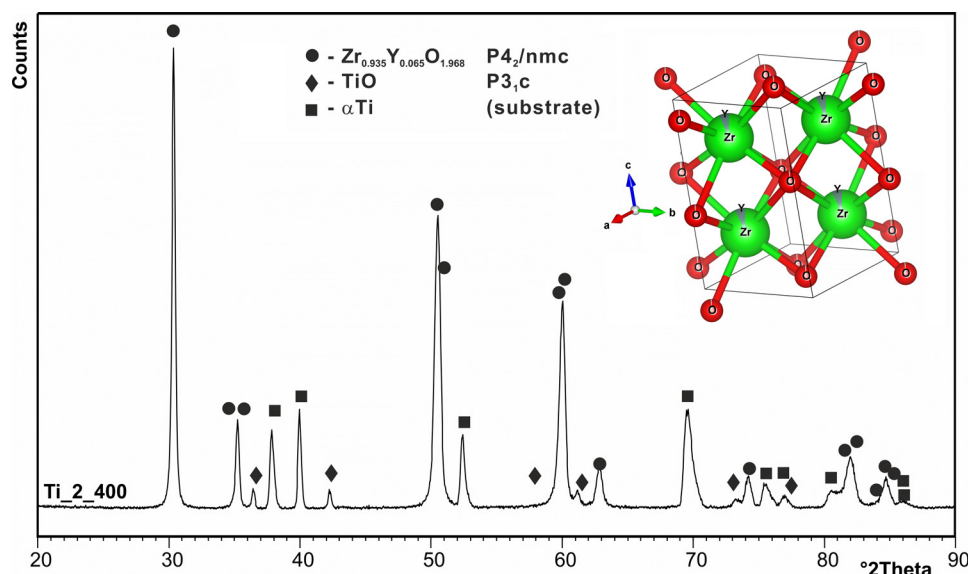


Fig. 1. X-ray pattern of coating with the simulation of a unit cell of the coating

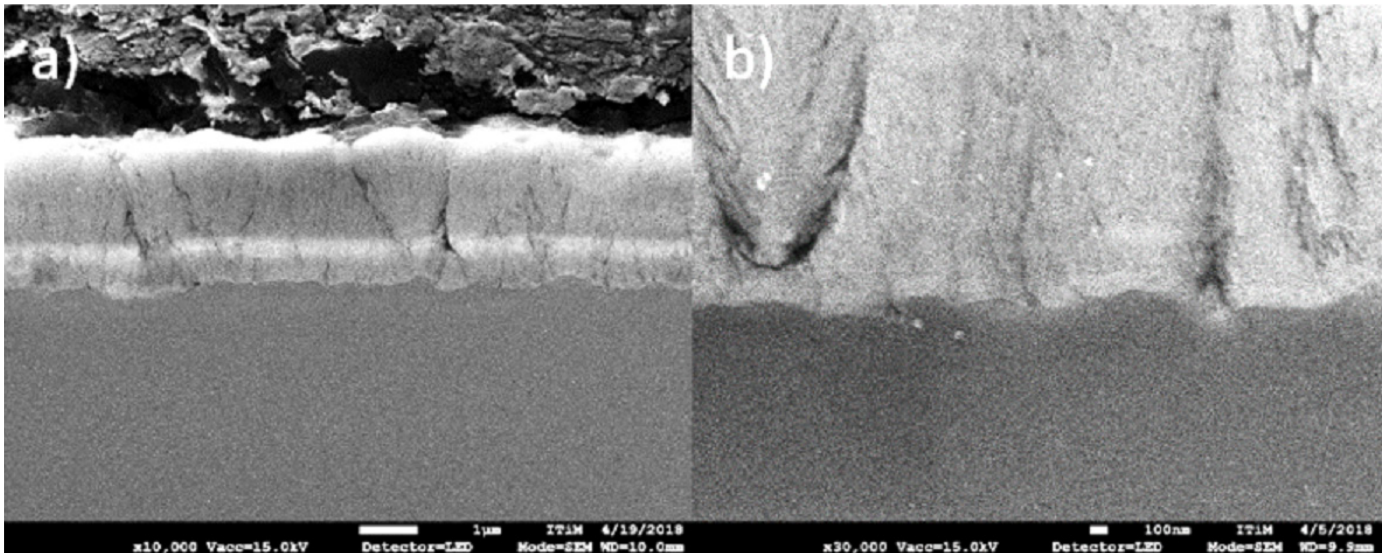


Fig. 2. Cross-section of a YSZ coating; scale bar: a) 1 μm b) 100 nm

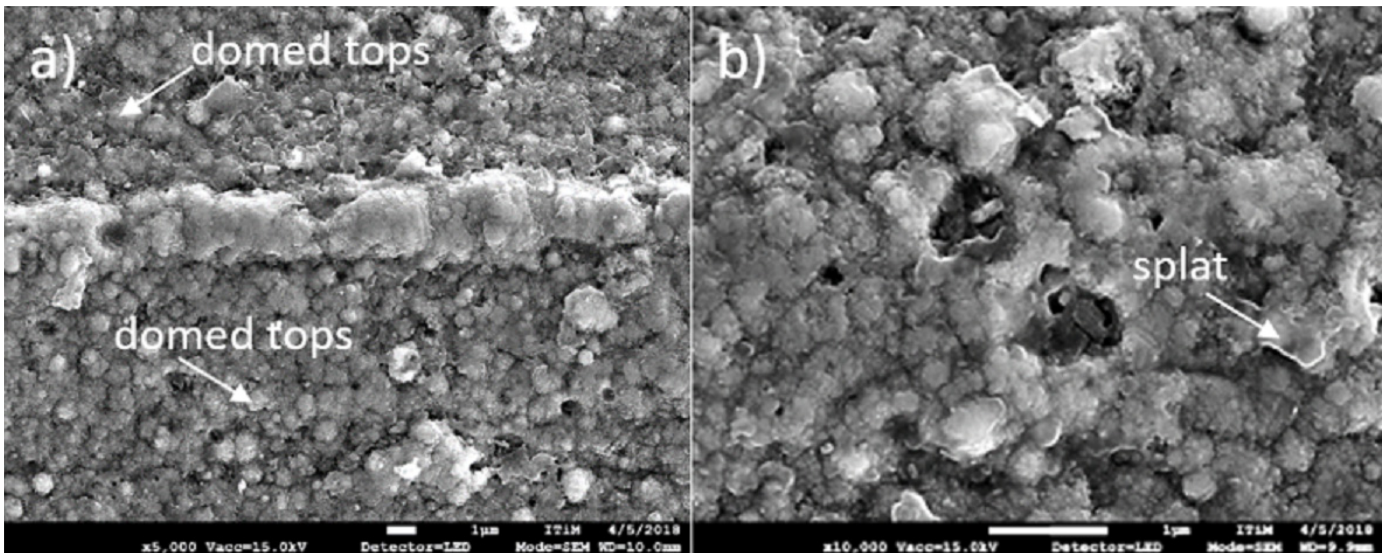


Fig. 3. Microphotograph of the surface of coating scale bar: a) 1 μm b) 1 μm

Surface images illustrate varied surface of the coating. Besides to domed tops, the surface shows porosity. The domed tops and pores presented on the surface have an impact on the roughness of the deposited coating. The profilometer test showed R_A equal to 0.40 μm . Other basic parameters of the surface are summarized in Table 2. As is known, the micro-, micro- and nanoroughness are distinguished. Each of them is associated with a different ability to osseointegrate. The resultant roughness (R_a) result of the tested sample equal to 0.40 μm , according to the works [10-12], is included in the nanoroughness. In accordance with the work Ehrenfest D. and et al. [10] nanoroughness increases surface energy which is associated with a significant increase in protein adsorption, bone cell proliferation and migration. Each of these roughnesses are important, but the most important is to find the optimal value according to the specific purpose. Further work will be carried out towards their optimization. It is worth adding that the result $R_a = 0.40 \mu\text{m}$ is twice as large as

compared to pure Ti [11,12]. Moreover, between the individual columns there are splats present in the form of discs of varying diameters. Splats are formed as a result of the rapid melting of the powder in the plasma stream and accelerated at high speed. Consequently, the drops hit and break at a huge speed on the substrate and solidify [13,14]. The presence of pores and domes of the vertices causes the development of the surface which is extremely important from the medical point of view, because the potential contact area of the implant with the bone is significantly increased [15]. It's known that greater roughness promotes differentiation of the cells and subsequent mineralization [16].

The distributions maps of elements for the obtained coatings revealed all the expected elements, i.e. yttrium, zirconium and titanium in the respective areas. Moreover, the presence of impurities was excluded. Figure 4 (overlap) shows the diffusion zone formed between the coating and the metal substrate. The examined material did not show delamination, accordingly the

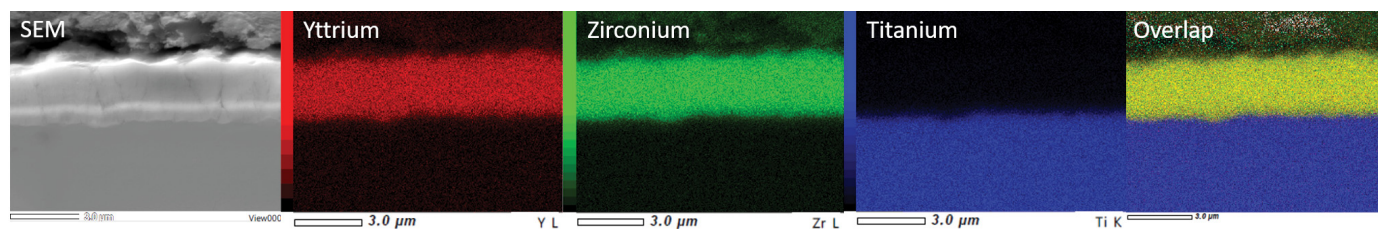


Fig. 4. An image of the distribution of elements obtained from HR-SEM EDS

coating shows good adhesion to the substrate, and the generated transition zone can have a significant impact on the lack of delamination.

Table 3 shows the hardness and Young's modulus respectively for the substrate and coating. In the case of hardness, it can be seen that the process of coating formation causes a slight increase in the value from 6.0(4) GPa to 7.0(1) GPa. In contrast, the spray coating reduces Young's modulus to 91(7) GPa. It is important because further research will be aimed at optimizing the discussed parameters in terms of biomedical aspects. All the more so because Shao and colleagues [17] showed changes in hardness and Young's modulus in the PS-PVD process with changes in parameters such as spray time and substrate distance from the plasma gun. According to the knowledge in the literature, the cp-Ti Young module has about 110 GPa [18,19]. In addition, the substrate achieves slightly higher values in the test material (133(2) GPa). However, from the medical point of view it is still a great difference when compared to the human bone module (~30 GPa) [18,20]. Therefore, the above studies allow us to continue further work related to the reduction of Young's modulus on materials for potential application as implants.

TABLE 3

Determined hardness and reduced Young's modulus for the substrate and coating

Sample	Substrate		Coating	
	Hardness [GPa]	Reduced Young's Modulus [GPa]	Hardness [GPa]	Reduced Young's Modulus [GPa]
Ti_2_400	6.0(4)	133(2)	7.0(1)	91(7)

4. Conclusion

- The PS-PVD method allows to obtain a YSZ coating on titanium substrate.
- Splats, gaps and pores, which are a consequence of the column structure, contribute to the differentiation of the surface of the coating.
- The coating produced causes a decrease in the Young's modulus of titanium substrate.
- Future work will investigate additional factors such as the influence of biomedical substrate and the effect of processing variables on thickness, topography and roughness.

REFERENCES

- [1] S.L. Aktug, I. Kutbay, M. Usta, Characterization and formation of bioactive hydroxyapatite coating on commercially pure zirconium by micro arc oxidation, *J. Alloys Compd.* (2017). doi:10.1016/j.jallcom.2016.10.217.
- [2] S. Madeira, A.M.P. Pinto, L.C. Rodrigues, O. Carvalho, G. Miranda, R.L. Reis, J. Caramês, F.S. Silva, Effect of sintering pressure on microstructure and mechanical properties of hot-pressed Ti6Al4V – ZrO₂ materials, *Mater. Des.* **120**, 394-403 (2017). doi:10.1016/j.matdes.2017.02.038.
- [3] R.I.M. Asri, W.S.W. Harun, M. Samykano, N.A.C. Lah, S.A.C. Ghani, F. Tarlochan, M.R. Raza, Corrosion and surface modification on biocompatible metals: A review, *Mater. Sci. Eng. C.* **77**, 1261-1274 (2017). doi:10.1016/j.msec.2017.04.102.
- [4] R.B. Osman, M. V. Swain, A critical review of dental implant materials with an emphasis on titanium versus zirconia, *Materials (Basel)* **8**, 932-958 (2015). doi:10.3390/ma8030932.
- [5] C. Song, M. Liu, Z.-Q. Deng, S.-P. Niu, C.-M. Deng, H.-L. Liao, A novel method for in-situ synthesized TiN coatings by plasma spray-physical vapor deposition, *Mater. Lett.* **217**, 127-130 (2018). doi:10.1016/J.MATLET.2018.01.068.
- [6] G. Mauer, A. Hospach, R. Vaßen, Process development and coating characteristics of plasma spray – PVD, *Surf. Coatings Technol.* **220**, 219-224 (2013). doi:10.1016/j.surfcoat.2012.08.067.
- [7] M. Góral, T. Kubaszek, S. Kotowski, J. Sieniawski, S. Dudek, Influence of deposition parameters on structure of TBCS deposited by PS-PVD method, *Int. Sci. Conf. Corros.* **227**, 369-372 (2015). doi:10.4028/www.scientific.net/SSP.227.369.
- [8] K. Szymański, M. Góral, T. Kubaszek, P.C. Monteiro, Microstructure of TBC Coatings Deposited by HVAF and PS-PVD Methods, *Solid State Phenom.* **227**, 373-376 (2015). doi:10.4028/www.scientific.net/SSP.227.373.
- [9] G. Mauer, A. Hospach, N. Zotov, R. Vaßen, Process conditions and microstructures of ceramic coatings by gas phase deposition based on plasma spraying, *J. Therm. Spray Technol.* **22**, 83-89 (2013). doi:10.1007/s11666-012-9838-y.
- [10] D.M. Dohan Ehrenfest, P.G. Coelho, B.S. Kang, Y.T. Sul, T. Albrektsson, Classification of osseointegrated implant surfaces: Materials, chemistry and topography, *Trends Biotechnol.* **28**, 198-206 (2010). doi:10.1016/j.tibtech.2009.12.003.
- [11] L. Le Guéhennec, A. Soueidan, P. Layrolle, Y. Amouriq, Surface treatments of titanium dental implants for rapid osseointegration, *Dent. Mater.* **23**, 844-854 (2007). doi:10.1016/j.dental.2006.06.025.

- [12] Y. Shibata, Y. Tanimoto, A review of improved fixation methods for dental implants. Part I: Surface optimization for rapid osseointegration, *J. Prosthodont. Res.* **59**, 20-33 (2015). doi:10.1016/j.jpor.2014.11.007.
- [13] B. Zhang, L. Wei, H. Guo, H. Xu, Microstructures and deposition mechanisms of quasi – columnar structured yttria – stabilized zirconia coatings by plasma spray physical vapor deposition, *Ceram. Int.* **43**, 12920-12929 (2017). doi:10.1016/j.ceramint.2017.06.190.
- [14] L. Gao, L. Wei, H. Guo, S. Gong, H. Xu, Deposition mechanisms of yttria-stabilized zirconia coatings during plasma spray physical vapor deposition, *Ceram. Int.* **42**, 5530–5536 (2016). doi:10.1016/j.ceramint.2015.12.111.
- [15] G.X. Tang, R.J. Zhang, Y.N. Yan, Z.X. Zhu, Preparation of porous anatase titania film, *Mater. Lett.* **58**, 1857-1860 (2004) . doi:10.1016/j.matlet.2003.11.016.
- [16] R. Agarwal, A.J. García, Biomaterial strategies for engineering implants for enhanced osseointegration and bone repair, *Adv. Drug Deliv. Rev.* **94**, 53-62 (2015). doi:10.1016/j.addr.2015.03.013.
- [17] F. Shao, H. Zhao, C. Liu, X. Zhong, Y. Zhuang, J. Ni, S. Tao, Dense yttria – stabilized zirconia coatings fabricated by plasma spray-physical vapor deposition, *Ceram. Int.* **43**, 2305-2313 (2017). doi:10.1016/j.ceramint.2016.11.014.
- [18] Y. Li, C. Yang, H. Zhao, S. Qu, X. Li, Y. Li, New Developments of Ti-Based Alloys for Biomedical Applications, 1709-1800 (2014). doi:10.3390/ma7031709.
- [19] J.M. Cordeiro, V.A.R. Barao, Is there scientific evidence favoring the substitution of commercially pure titanium with titanium alloys for the manufacture of dental implants?, *Mater. Sci. Eng. C* **71**, 1201-1215 (2017). doi:10.1016/j.msec.2016.10.025.
- [20] M. Long, H.J. Rack, Titanium alloys in total joint replacement – a materials science perspective, *Biomaterials* **19**, 1621-1639 (1998). doi:10.1016/S0142-9612(97)00146-4.